Preliminary Investigation of the UV LED Photodegradation of Methylene Blue Using TiO_2–carbonized Medium-density Fiberboard

Justin Alfred Pe III,[a] Sung Phil Mun,[a,*] and Jae Pil Kim [b]

This preliminary study aimed to realize the potential use of titanium dioxide–carbonized medium-density fiberboard (TiO_2–cMDF) as a biomaterial for dye wastewater treatment. TiO_2–cMDF, which was prepared by carbonizing MDF treated with titanium tetraisopropoxide in isopropyl alcohol, was investigated for adsorption and then photodegradation of methylene blue (MB) under UV-A (390 nm, 19 W) and UV-C (280 nm, 12 W) light emitting diodes (LEDs). After two full cycles of adsorption, four successive cycles of photodegradation were conducted under UV-A LED. For every adsorption or photodegradation cycle, TiO_2–cMDF practically removed MB. Both adsorption and photodegradation followed pseudo-first-order kinetics. The rate constants for adsorption decreased by half. The rate constants for photodegradation were similar. This finding suggests that UV-A LED is a robust and steady source of UV light. Photodegradation under UV-C LED was also performed. However, due to its high-energy output, the UV-C LED module overheated even though a cooling fan was present. Although the results indicate a slow photodegradation under UV LEDs, because of the limited number of specimens, increasing the number of specimens and UV LED modules will improve its performance.

DOI: 10.15376/biores.17.3.4595-4606

Keywords: Medium-density fiberboard; Carbonization; Photodegradation; Methylene blue; UV LED

*Contact information: a: Department of Wood Science and Technology, Jeonbuk National University, Jeonju, 54896 South Korea; b: Mobility Lighting Research Center, Korea Photonics Technology Institute, Gwangju, 61007 South Korea; *Corresponding author: msp@jbnu.ac.kr*

INTRODUCTION

Various industries, such as textile, dyeing, pulp and paper, tannery and paint, and dye manufacturing, are responsible for the discharge of dye effluents in wastewater systems (Katheresan *et al*. 2018). These industries release colored wastewater due to the consumption of various kinds of natural or synthetic dyes, many of which contain complex aromatic structures that are difficult to decompose. Synthetic dyestuffs, such as methylene blue (MB), must be removed from wastewater systems because they impart color, cause harmful environmental effects even in low concentrations (Pandey *et al*. 2007), and promote adverse effects on the central nervous system (Vutskits *et al*. 2008). However, existing wastewater treatments are quite unsatisfactory and need a step of further purification. Water treatments through advanced oxidation processes (AOPs), such as ozone-based, ultra violet (UV)-based, and Fenton-based AOPs, are common in the removal of inorganic and organic pollutants (Deng and Zhao 2015). Currently, UV-based AOPs using titanium dioxide (TiO_2) as catalyst are widely utilized in drinking water and wastewater treatments (Miklos *et al.* 2018). A majority of these UV/TiO_2 AOPs prefer TiO_2 suspensions rather than TiO_2 immobilized in a support. The TiO_2 suspensions have closer proximity between surface and pollutant (Simonsen 2014). However, suspended TiO_2 particles can affect the transmission of UV light by blocking or shading other TiO_2 particles, which can result in decreased photocatalytic efficiency. This problem in UV/TiO_2 AOPs can be solved by immobilizing TiO_2 onto support materials. In addition, if the support enhances the surface area, maintains catalytic function, offers strong adherence between catalyst and support, and shows strong adsorption affinity with pollutants (Shan *et al.* 2010), then, immobilizing TiO_2 onto a support provides additional functionality.

Wood-based materials were selected as support materials for TiO_2 because the surface areas were remarkably improved. In addition, the TiO_2-decorated bleached wood by He *et al.* (2019) had comparable catalytic function or even better photocatalytic degradation at 40 and 60 ppm (mg/L) than that of TiO_2 suspensions. The authors' previous work on TiO_2–carbonized medium-density fiberboard (TiO_2–cMDF) exhibited strong adherence between catalyst and support, and showed satisfactory dye removal properties due to higher adsorption affinity and photodegradation (Pe *et al.* 2021). Photodegradation of MB using TiO_2–cMDF, with a UV-C (254 nm) lamp immersed in the dye solution, practically removed MB. However, the UV-C lamp consumes more power, generates more heat, and is unsuitable for large-scale designs. Today, commercial UV LEDs are more energy-efficient, long lasting, provide a consistent light source, and are thermoelectrically controlled (Muramoto *et al.* 2014). Thus, UV LEDs are utilized as photon sources of UV light for the heterogeneous photocatalytic oxidation of organic pollutants (Levine *et al.* 2011). In this work, the UV LEDs were used as light sources and were fixed above the MB solution. This means that the UV light produced travelled from two different media (air to water) in contrast to the previous work done by the authors. Several works involving the photodegradation of dyes under TiO_2/UV LEDs systems have been reported (Tayade *et al.* 2009; Natarajan *et al.* 2019). Despite the high photocatalytic activities of the reported TiO_2/UV LED systems, commercialization/large-scale applications might not be practical. Thus, the purpose of this study was to investigate the adsorption and photodegradation of MB dye using TiO_2 immobilized in carbonized MDF under UV-A and UV-C LEDs for a practical efficacy in dye wastewater treatment.

EXPERIMENTAL

Materials

The UV-A (390 nm, 19 W) and UV-C (280 nm, 12 W) LED modules were provided by the Korea Photonics Technology Institute (KOPTI, Gwangju, Korea). The TiO_2–cMDF panel was previously prepared and provided kindly by Lee *et al.* (2019b).

Methods

Preparation of TiO_2–cMDF

The preparation of TiO_2–cMDF is shown in Fig. 1. A photocatalyst precursor titanium tetraisopropoxide (Ti-tip, Daejung Chemicals, Siheung, Korea) was dissolved in 50% (v/v) isopropyl alcohol (IPA) (Daejung Chemicals, Siheung, Korea). Approximately 7 g of 50% Ti-tip solution was equally applied on the surface of MDF specimens of dimensions 260 mm (L) × 100 mm (W) × 7 mm (T) (Sunchang Industry, Incheon, Korea) *via* brush coating method. The 50% Ti-tip-treated MDFs were air-dried in a fume hood and further dried in a convection oven at 60 °C for 3 h. The dry Ti-tip-treated MDFs were carbonized in an electric furnace with a thermal schedule of 50 °C/h to 700 °C for 2 h.

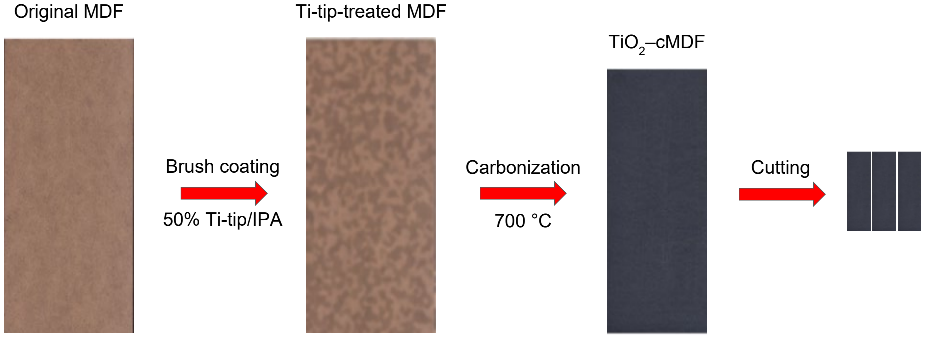

Fig. 1. Preparation of the TiO_2–cMDF panel and specimens

Crystallinity of TiO_2–cMDF

The TiO_2 crystalline structure on the surface of TiO_2–cMDF was determined by powder X-ray diffraction (XRD, D/Max-2500, Rigaku, Japan) using Cu Kα radiation (λ = 1.5406 Å) under the conditions of 40 kV and 30 mA from the starting angle. The XRD spectrum was processed and compared to a TiO_2 reference spectrum.

Evaluation for the adsorption of MB

The resulting TiO_2–cMDF panel prepared using the above method was cut into specimens of dimensions 60 mm (L) × 20 mm (W) × 3 mm (T). Three TiO_2–cMDF specimens were fixed on a stainless-steel support with a polyethylene hot-melt adhesive. The specimens were then immersed in 275 mL of 10 ppm MB (Yakuri Pure Chemicals, Kyoto, Japan) solution in a 300-mL glass dish under magnetic stirring at room temperature (25±2 °C). A full cycle of adsorption was completed upon reaching 99% removal of MB. After one full cycle of adsorption, the solution was discarded and a fresh batch of 275 mL of 10 ppm MB solution was added to carry out another cycle of adsorption. Figure 2 shows the representation of the adsorption experiment.

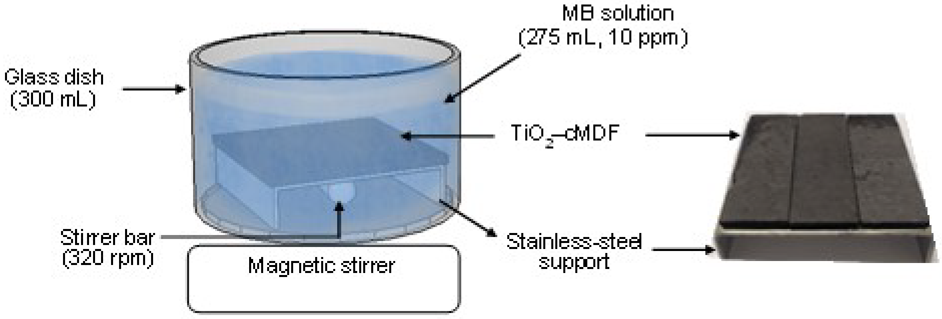

Fig. 2. Representation of the adsorption experiment

The decrease in spectral absorption at 665 nm monitored by a visible spectrophotometer (Optizen 3220, Mecasys, Seoul, Korea) indicated the removal of MB, following Eq. 1,

$$\text{MB removal (\%)} = [(C_o - C_t) / C_o] \times 100 \tag{1}$$

where C_o is initial concentration (ppm) and C_t denotes the concentration (ppm) at time t (h).

The non-linear plots of the MB removal were transformed into linear plots using either normalization through exponential (Eq. 2) or hyperbolic (Eq. 3) functions designed for pseudo-first-order or pseudo-second order kinetics, respectively. The rate constants were estimated by calculating the slopes of the following Eqs. 2 and 3,

$$\ln C_t = \ln C_o - k_1 t \tag{2}$$

$$(1/C_t) = (1/C_o) + k_2 t \tag{3}$$

where k_1 is pseudo-first-order rate constant (1/h), k_2 is pseudo-second-order rate constant (1/ppm·h), and t is time (h).

Evaluation for the photodegradation of MB

After the second cycle of adsorption, the solution was discarded and the same amount of fresh MB solution was again added. Afterwards, a UV-A LED module attached on an aluminum heatsink with a cooling fan was placed on top of a plate with a square hole. The distance between the UV-A LED and the TiO_2–cMDF was 28 mm, which means that approximately 67% of the UV light would be absorbed by the medium before reaching the specimen. That means, only 33% of the UV light was transmitted efficiently to the TiO_2–cMDF surface. The UV-A LED module was connected to a DC regulated power supply and operated at 8.0 V and 600 mA. Similarly, another experiment was performed using a UV-C LED module and was operated at 15.0 V and 200 mA. The water lost due to evaporation was periodically replenished. Figure 3 shows a schematic representation of the photodegradation experiment.

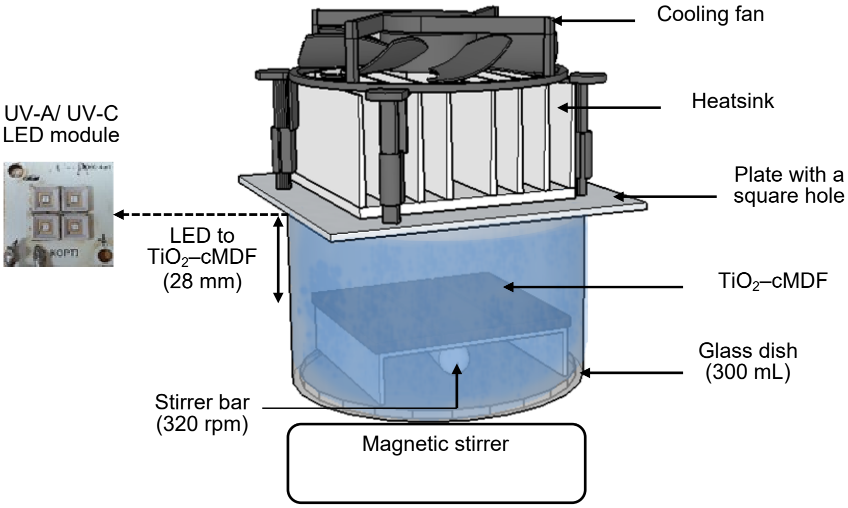

Fig. 3. Representation of the photodegradation experiment

The photodegradation of MB was performed in four cycles. The photodegradation cycle under a UV LED module was deemed completed when MB removal reached 99%. The MB solution after each cycle of photodegradation was discarded and a same amount of fresh MB solution was used each time. Similarly, the removal of MB and their respective kinetics were evaluated using Eqs. 1-3.

Titanium distribution on the surface and cross-section of TiO_2–cMDF specimens

After the experiment, three TiO_2–cMDF specimens were subjected to surface analysis along with an untreated TiO_2–cMDF (not subjected to adsorption and photodegradation). The Ti distribution and elemental content on the TiO_2–cMDF surfaces were obtained using scanning electron microscopy energy-dispersive spectroscopy (SEM-EDS) (Supra 40VP, Carl Zeiss AG, Oberkochen, Germany) at the Center for University-wide Research Facility, Jeonbuk National University. The surface images were taken at 350× magnification. A total of 27 data points (three equidistant spots per specimen and three different SEM scans per spot) were collected for elemental analysis. The determination of Ti distribution and Ti layer thickness were conducted on the cross-section of an untreated TiO_2–cMDF at 40× magnification.

RESULTS AND DISCUSSION

Specialty wood composites, such as cMDFs and TiO_2–cMDFs, were manufactured using a pressing carbonization method to produce a porous, crack-, and twist-free carbonized fiberboard (Park *et al*. 2009). The dimensional changes and weight reductions within the fiberboards (cMDFs and TiO_2–cMDFs) at several carbonization temperatures were reported (Lee *et al*. 2019a). Specifically, for the TiO_2–cMDF prepared at 700 °C, about 57.3% and 70.4% decrease in volume and weight, respectively, were noted. The decrease in volume and weight were primarily due to the fibreboard, since the amount of Ti-tip added was not affected. The crystallinity, adsorption characteristics, and photodegradation performance of TiO_2–cMDF are described.

Crystallinity of TiO_2–cMDF

Figure 4 shows the XRD spectrum of TiO_2–cMDF carbonized at 700 °C. The XRD peaks of TiO_2–cMDF are in agreement with the typical peaks of anatase-type TiO_2 at 2θ values of 25.3°, 36.9°, 37.8°, 38.6°, 48.0°, 53.9°, 55.1°, 62.1°, 62.7°, 68.8°, 70.3°, 74.0°, 75.0°, and 76.0° (JCPDS Card no. 21-1272).

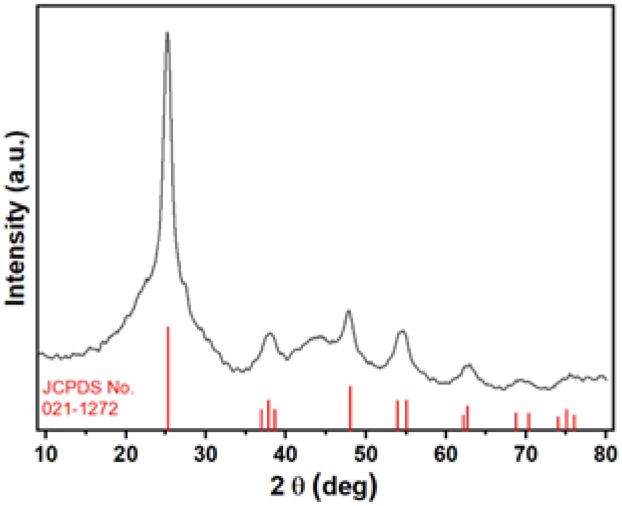

Fig. 4. XRD spectrum of TiO_2–cMDF along with TiO_2 anatase reference

Figure 5 represents the transformation of Ti-tip precursor to anatase-type TiO_2. Anatase was the preferred crystalline structure of the Ti-tip-treated cMDF carbonized in the range 600 to 900 °C; carbonization beyond 900 °C results to the formation of rutile (Lee *et al*. 2019a).

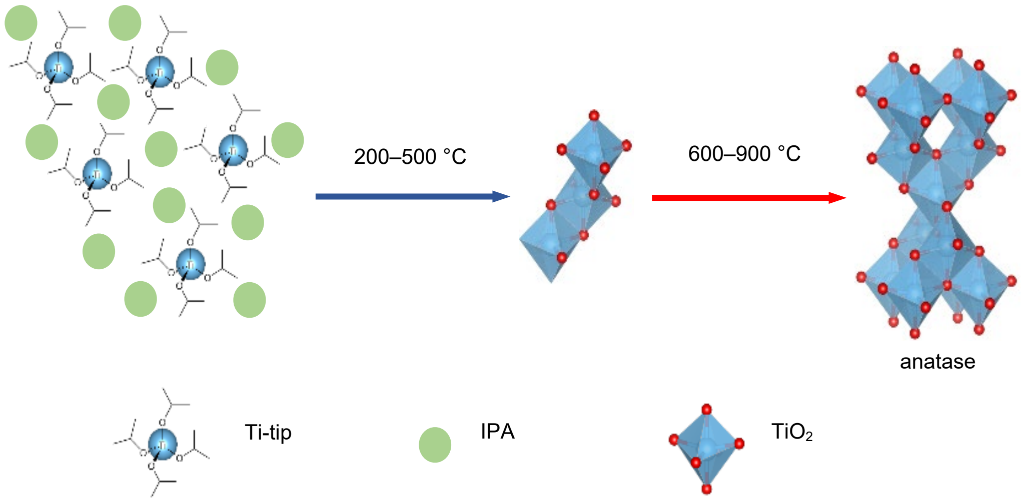

Fig. 5. Graphical representation for the formation of anatase TiO_2

Adsorption Characteristics of MB on TiO_2–cMDF

Carbonized wood-based materials prepared from ash (*Fraxinus* sp.) board, MDF, oriented strand board, particleboard, and plywood exhibited Brunauer–Emmett–Teller (BET) surface areas ranging from 360 m^2/g to 850 m^2/g (Lee *et al*. 2017). For TiO_2–cMDFs, the BET surface area ranged from 100 m^2/g to 500 m^2/g (Mun and Park 2011). Considering the abilities of carbonized wood-based materials to adsorb organic compounds due to their high surface areas, TiO_2–cMDF was treated with MB solution to achieve two full adsorption cycles. The first adsorption cycle was completed in 462 h upon reaching 99% removal of MB, while the second adsorption cycle took longer time. Adsorption was discontinued after two cycles because another cycle will require much longer times. Nonetheless, a complete adsorption was not yet achieved and will affect the results of photodegradation. The rate constant dropped 48% from the first to second cycle of adsorption as the available sites for adsorption were decreased. The mechanism of MB removal was through adsorption on the surface of TiO_2–cMDF and diffusion through the crevices of TiO_2–cMDF. Normalization of the graph in Fig. 6a using Eqs. 2 and 3 indicated that both adsorption cycles followed pseudo-first-order kinetics (Fig. 6b) rather than pseudo-second-order kinetics.

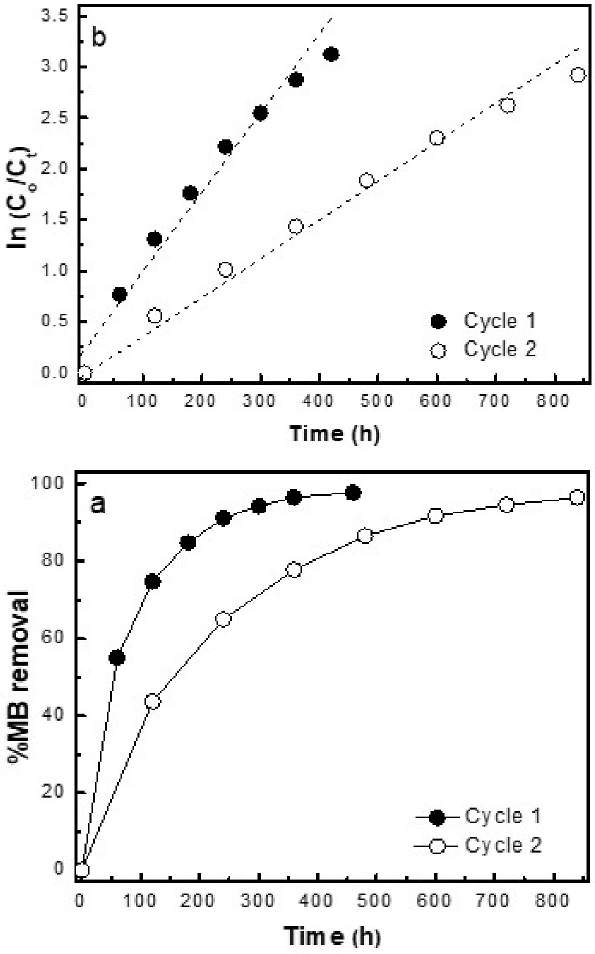

Fig. 6. Adsorption kinetics of MB: a) MB removal (%); and b) pseudo-first-order plot

Photodegradation Characteristics of MB on TiO_2–cMDF

Photodegradation was performed in four cycles. Figure 7 indicates that photodegradation of MB followed pseudo-first-order kinetics.

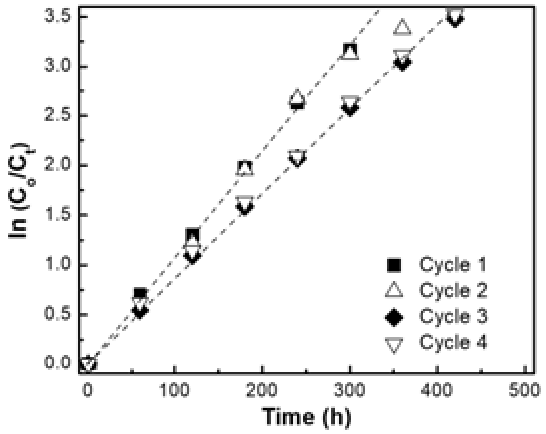

Fig. 7. Photodegradation kinetics of MB (pseudo-first-order plot)

Table 1. Kinetics of MB Removal Through Adsorption and Photodegradation

Phase	Cycle	Rate Constant (× 10^{-3}/h)	t_{99} (h)	t_{99} (d)
Adsorption	1	6.7	462	19.25
	2	3.5	864	36.0
Photodegradation	1	10.3	348	14.5
	2	10.0	372	15.5
	3	8.4	420	17.5
	4	8.2	420	17.5

In Table 1, the photodegradation rate constants for the first and second cycles were similar. The photodegradation rate constants for the third and fourth cycles were similar as well. However, because a complete adsorption was not yet reached, the photodegradation rate constants for the first and second cycles might be affected. Based from the trend of adsorption rate constants, a third adsorption cycle is possible and the rate constant can be estimated as 1.6 × 10^{-3}/h. Presumably, the rate constants for the first and second cycles are within 8.0 × 10^{-3}/h to 9.0 × 10^{-3}/h due to the inherent effects of adsorption. For the third and fourth cycles, the effect of adsorption might be minimal. A cycle of photodegradation occurred in the range of 348 to 420 h (15 to 18 days) with attainment of 99% removal of MB. Photodegradation of MB was monitored by the decrease in the intensity of visible absorption peak at the maximum wavelength (λ_{max}) at 665 nm.

Figure 8 shows the changes in the spectral absorption recorded for the first cycle. From the graph, a deviation from the λ_{max} was observed as more MB was removed. This shift in wavelength can be attributed to the degradation of MB. Because the specimens were submerged in aqueous medium for the entire experimental period, a concern that some TiO_2 may be removed from the surface of TiO_2–cMDF was recognized. Thus, ion distribution by EDS was determined on the cross-section and surface of TiO_2–cMDF to estimate the Ti distribution and elemental content. Cross-sectional SEM and Ti distribution images of an untreated TiO_2–cMDF are also shown in Fig. 9. The results of the EDS showed that the initial Ti layer was 0.75 mm thick, which indicated that there were sufficient photocatalytic sites on the TiO_2–cMDF surface.

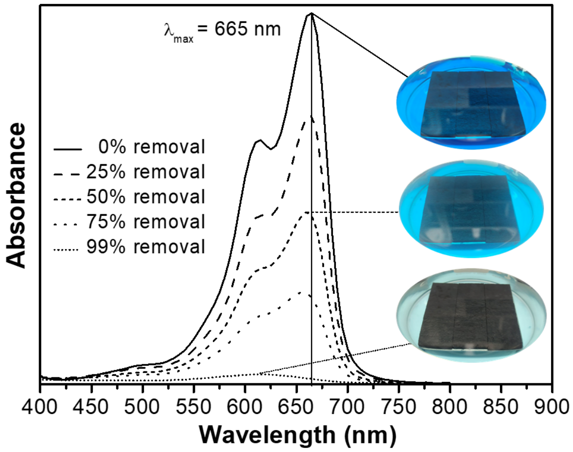

Fig. 8. Changes in spectral absorptions of MB

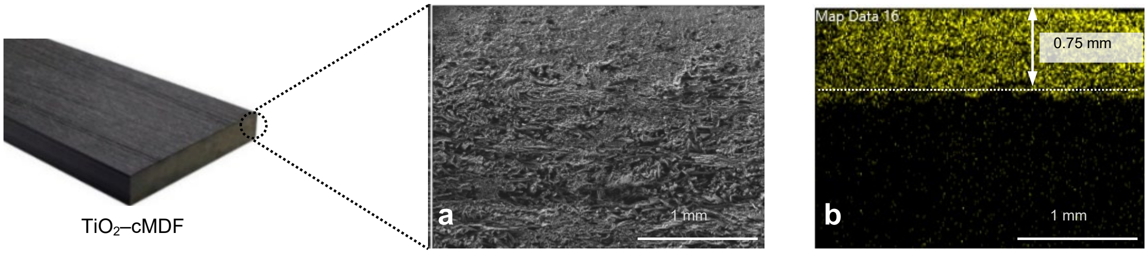

Fig. 9. Cross-sectional images: a) SEM image; and b) Ti distribution of an untreated TiO_2–cMDF

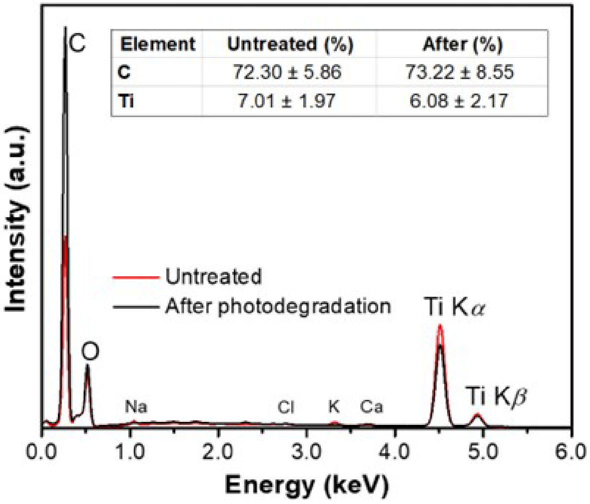

Element	Untreated (%)	After (%)
C	72.30 ± 5.86	73.22 ± 8.55
Ti	7.01 ± 1.97	6.08 ± 2.17

Fig. 10. EDS spectra of TiO_2–cMDF surface: Untreated and after photodegradation

In Fig. 10, the Ti content on the surface of TiO_2–cMDF was reduced by a small amount. Figure 11a shows an untreated surface of TiO_2–cMDF wherein the yellow color represents Ti. After six (two adsorption and four photodegradation) cycles, the TiO_2–cMDF was covered with carbon materials, the red color, which originated from MB degradation (Fig. 11b). These findings can explain the increase in C content and decrease in Ti content observed in EDS. The photocatalytic properties of TiO_2–cMDF can be restored by re-carbonization at 700 °C. The carbon materials adsorbed on the surface can be removed through thermal oxidation. At the same time, the TiO_2 on the surface should retain their anatase crystalline structure.

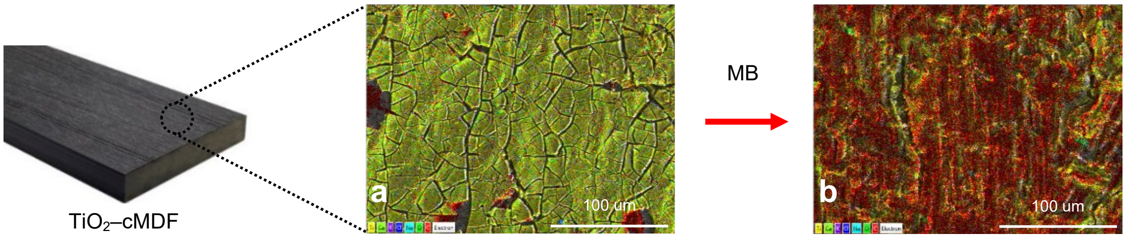

Fig. 11. Elemental distribution on the TiO_2–cMDF surface: a) Untreated; and b) after photodegradation

Optical properties of UV-A LED

After four cycles of photodegradation (total runtime of 1560 h), the radiant power of the used UV-A LED was compared to a new UV-A LED over the wavelength range of 300 to 700 nm. The results confirmed that the radiant power slightly decreased 7% (Fig. 12). An additional test in terms of the input current at 600 mA confirmed a 100 mW decrease (Fig. 12 inset). Based on these optical results, UV-A LED is considered a robust and a steady source of UV light for MB photodegradation.

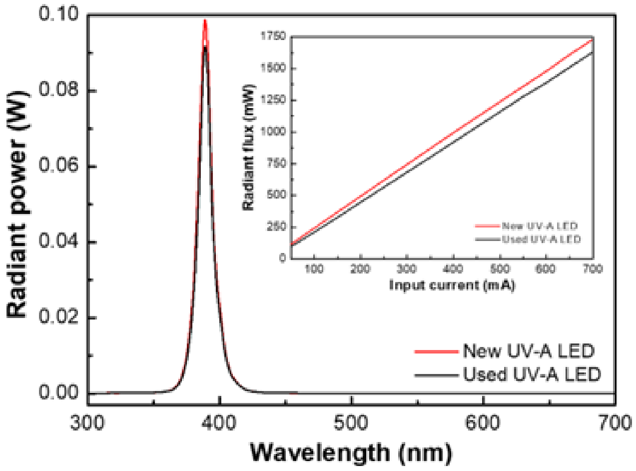

Fig. 12. Radiant power and wavelength distribution of UV-A LED

Comparison of photodegradation under different UV LEDs

A similar experiment was conducted using one UV-C LED module. The first cycles of photodegradation under UV-A and UV-C LED are compared in Fig. 13. At t = 60 h, UV-A removed 50% of MB while UV-C removed 37% of MB dye. However, at t = 300 h, both UV LEDs removed the same amount of MB. Although, the UV-A and UV-C LEDs removed the same amount of MB dye at a certain time, the rate constant for UV-A (10.3×10^{-3}/h) was higher than that for UV-C (3.5×10^{-3}/h). Unfortunately, only one cycle of photodegradation was performed because the UV-C LED overheated due to its high-energy output despite the presence of a cooling fan.

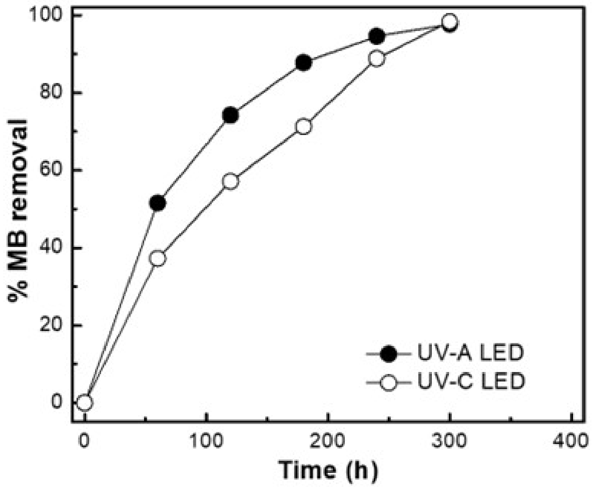

Fig. 13. Photodegradation under UV-A and UV-C LEDs

CONCLUSIONS

1. TiO_2–cMDF practically removed methylene blue (MB) dye through adsorption and photodegradation under UV-A and UV-C LED light sources.
2. In the photodegradation of MB using TiO_2–cMDF, UV-A LED exhibited consistent and faster MB removal performance than UV-C LED. This demonstrates that UV-A LED is a robust and steady source of UV light for MB photodegradation.
3. Adsorption and photodegradation of MB followed pseudo-first-order kinetics. The rate constants for adsorption decreased by half after the first cycle of adsorption. The rate constants for photodegradation were similar.
4. Although the TiO_2–cMDF showed slow photodegradation, increasing the number of specimens and UV LED modules can improve the photocatalytic performance. As such, this simple set-up can be applied to large scale applications.
5. This preliminary study on TiO_2–cMDF for the photodegradation of MB under UV LEDs suggests that TiO_2–cMDF is a prospective biomaterial for practical dye wastewater treatment.

ACKNOWLEDGMENTS

The authors are thankful to Dr. Min Lee (Department of Wood Products, National Institute of Forest Science, Korea) for providing the TiO_2–cMDF panel.

REFERENCES CITED

Deng, Y., and Zhao, R. (2015). "Advanced oxidation processes (AOPs) in wastewater treatment," *Curr. Pollut. Rep.* 1, 167-176. DOI: 10.1007/s40726-015-0015-z

He, Y., Li, H., Guo, X., and Zheng, R. (2019). "Bleached wood supports for floatable, recyclable, and efficient three dimensional photocatalyst," *Catalysts* 9(2), article no. 115. DOI: 10.3390/catal9020115

Katheresan, V., Kansedo, J., and Lau, S. Y. (2018). "Efficiency of various recent wastewater dye removal methods: A review," *J. Environ. Chem. Eng.* 6(4), 4676-4697. DOI: 10.1016/j.jece.2018.06.060

Lee, M., Jang, J., Lee, S. M., and Park, S. B. (2017). "Comparison of the radon absorption capacity of carbonized boards from different wood-based panels," *BioResources* 12(3), 6427-6433. DOI: 10.15376/biores.12.3.6427-6433

Lee, M., Park, S. B., and Mun, S. P. (2019a). "One-step preparation of TiO_2-carbonized medium-density fiberboard for volatile organic compound photodegradation," *BioResources* 14(3), 5533-5543. DOI: 10.15376/biores.14.3.5533-5543

Lee, M., Park, S. B., and Mun, S. P. (2019b). "Synthesis of TiO_2 *via* modified sol-gel method and its use in carbonized medium-density fiberboard for toluene decomposition," *BioResources* 14(3), 6516-6528. DOI: 10.15376/biores.14.3.6516-6528

Levine, L. H., Richards, J. T., Coutts, J. L., Soler, R., Maxik, F., and Wheeler, R. M. (2011). "Feasibility of ultraviolet light emitting diodes as an alternative light source for photocatalysis," *J. Air Waste Manage*. 61(9), 932-940. DOI: 10.1080/10473289.2011.596746

Miklos, D. B., Remy, C., Jekel, M., Linden, K. G., Drewes, J. E., and Hubner, U. (2018). "Evaluation of advanced oxidation processes for water and wastewater treatment - A critical review," *Water Res*. 139, 118-131. DOI: 10.1016/j.watres.2018.03.042

Mun, S. P., and Park, S. B. (2011). "Preparation of the functionality enhanced carbonized medium density fiberboard by pretreatment of photocatalyst precursor, titanium tetraisopropoxide," in: *Poster presentation*, *Forest Products Society*, 65th International Convention, Portland, OR, USA, pp. 127.

Muramoto, Y., Kimura, M., and Nouda, S. (2014). "Development and future of ultraviolet light emitting diodes: UV LED will replace the UV lamp," *Semicond. Sci. Technol*. 29(8), article ID 084004. DOI: 10.1088/0268-1242/29/8/084004

Natarajan, K., Natarajan, T. S., Bajaj, H. C., and Tayade, R. J. (2019). "Rutile phase dominant TiO_2 formed by thermal treatment and its high photocatalytic activity under narrow spectrum ultraviolet light emitting diodes," *Mater. Res. Express*. 6(1), 1-15. DOI: 10.1088/2053-1591/aae861

Pandey, A., Singh, P., and Iyengar, L. (2007). "Bacterial decolorization and degradation of azo dyes," *Int. Biodeter. Biodegr.* 59(2), 73-84. DOI: 10.1016/j.ibiod.2006.08.006

Park, S. B., Lee, S. M., Park, J. Y., and Lee, S. H. (2009). "Manufacture of crack-free carbonized board from fiberboard," *Mokchae Konghak* 37(4), 293-299.

Pe, J. A., Mun, S. P., and Lee, M. (2021). "TiO_2-carbonized medium-density fiberboard for the photodegradation of methylene blue," *Wood Sci. Technol*. 55(4), 1109-1122. DOI: 10.1007/s00226-021-01308-3

Shan, A. Y., Ghazi, T. I. M., and Rashid, S. A. (2010). "Immobilisation of titanium dioxide onto supporting materials in heterogeneous photocatalysis: A review," *Appl. Catal. A-Gen.* 389(1-2), 1-8. DOI: 10.1016/j.apcata.2010.08.053

Simonsen, M. E. (2014). "Heterogeneous photocatalysis," in: *Chemistry of Advanced Environmental Purification Processes of Water*, E. G. Sogaard (ed.), Elsevier, Amsterdam, Netherlands, pp. 135-170. DOI: 10.1016/B978-0-444-53178-0.00004-3

Tayade, R. J., Natarajan, T. S., and Bajaj, H. C. (2009). "Photocatalytic degradation of methylene blue dye using ultraviolet light emitting diodes," *Ind. Eng. Chem. Res*. 48(23), 10262-10267. DOI: 10.1021/ie9012437

Vutskits, L., Briner, A., Klauser, P., Gascon, E., Dayer, A. G., Kiss, J. Z., Muller, D., Licker, M. J., and Morel, D. R. (2008). "Adverse effects of methylene blue on the central nervous system," *Anesthesiology* 108(4), 684-692. DOI: 10.1097/ALN.0b013e3181684be4

Article submitted: July 13, 2021; Peer review completed: August 21, 2021; Revised version received and accepted: June 12, 2022; Published: June 14, 2022.
DOI: 10.15376/biores.17.3.4595-4606